

Investigation of the Experimental and Theoretical Release of Caffeine from Cosmetic Hydrogels and Patches

Jiao, Yimeng^{1*}; Rakic, Aleksandra²; Janjic, Goran³; Tamburic, Slobodanka¹; Stevic, Milica¹

¹ Cosmetic Science Research Group, London College of Fashion, University of the Arts London, London, UK;

² Faculty of Physical Chemistry, University of Belgrade, Belgrade, Serbia;

³ Institute of Chemistry, Belgrade, Serbia.

* Yimeng Jiao, 20 John Prince's Street, London, UK, W1G 0BJ, +44 7453347444, y.jiao@fashion.arts.ac.uk

Abstract

Molecular docking (MD) is a tool that performs computational simulation. It can be used to predict the types of chemical interactions by calculating binding energies of temporary created complexes between the molecules. This study explores the applicability of MD by comparing experimental (IVRT) and theoretical (MD) release of caffeine from six different cosmetic hydrogels and patches. MD studies of caffeine and gelling agents (GAs) were performed by the Autodock Vina software. The GAs and caffeine structures were optimised by the Density Functional Theory (DFT) calculations. A Fused Deposition Modelling 3D printer (Ultimaker, UK) was used to fabricate polyvinyl alcohol (PVA), patches, which were loaded with six different caffeine-containing hydrogels, respectively. IVRT of caffeine from both hydrogels and patches was performed using vertical diffusion cells (Copley, UK) with cellulose acetate membrane, at 30 min, 1 h, 2 h, 3h, 5h, and 6 h.

The binding energy (BE) of a single neutral caffeine molecule with different GAs (**caffeine-GA**) was found to be from -2.4 to -4.1 kcal/mol, while the BE for the **membrane-GA** was from -4.1 to -6.8 kcal/mol. The BE for the **caffeine-membrane** system was -5.0 kcal/mol. The MD calculations on the membrane structure have shown that all GAs possess higher affinity towards membrane than towards caffeine. Furthermore, the caffeine affinity towards membrane was higher than towards any GA. However, the difference between these affinities (membrane-GA and caffeine-GA) is almost identical. Hence, the

MD results indicated that there would be no distinctive difference in caffeine kinetics among the hydrogels studied. This theoretical approach was supported by the IVRT results, which showed similar release profiles from the six hydrogels and the PVA-based patches loaded with those hydrogels, respectively. Therefore, this study has provided a 'proof of concept' that the *in vitro* release of caffeine from hydrogels could be predicted by using theoretical MD approach.

Keywords: topical delivery; hydrogel; molecular docking (MD); 3D printing; *in vitro* release.

Introduction

Hydrogel formulations are well established for their use in cosmetic products. They consist of active ingredients and gelling agents as the key excipients. Gelling agents are hydrophilic polymeric materials that form three-dimensional networks and are able to retain water molecules within the structure and expand, which is referred to as swelling. Their capacity for water absorption is due to the hydrophilic functional groups that are present in the polymer molecules. There are three states that water exist in a hydrogel: a) free water, which is mobile, without chemical bonding to the polymer functional groups; b) intermediate water that forms weak interactions with the polymer, and c) hydrogen-bonded water which do not undergo freezing [1]. The release of active ingredients from hydrogel formulations takes place through diffusion, affected by the hydrogel structure; and their rheological properties are known to affect release profiles [2].

Molecular docking (MD) is a widely used computational tool, which could provide a better understanding of the interactions in chemical systems [3]. MD predicts the most probable three-dimensional structure of the ligand and the target macromolecule, in addition to their conformations/orientations, followed by the calculation of the binding energy of each possible means of interaction, in order to predict the most probable type and location of binding [4].

In this study, MD calculations were performed on six hydrogel systems, which differ only in the type of gelling agent used, to find a potential candidate for the highest release of the

model active ingredient-caffeine. The gelling agents included both polysaccharide-based and synthetic polymeric materials, which have produced distinct rheological profiles.

Theoretical results were analysed against those obtained by the commonly used experimental method of in vitro release testing (IVRT) to test the applicability of the method. It was of interest to find out whether, and to which extent, the two sets of results would correlate.

Materials and Methods

Materials

Caffeine (Sigma-Aldrich, UK) was used as a model active ingredient. The preservative used in the formulations was methylparaben and the pH adjuster was citric acid. The six gelling agents used in this study are summarised in Table 1.

Polylactic acid (PLA) and natural polyvinyl alcohol (PVA) filaments were obtained from Ultimaker (Netherland); both were 2.85 mm in diameter. Cellulose acetate (CA) membrane (Whatman[®], DE) and a phosphate buffer solution (PBS) were used for in vitro release tests. PBS solution in the receptor phase of Franz cells simulates the fluid present in the epidermis. The cellulose acetate (CA) membrane acted as a barrier that separates the hydrogel and the PBS solution in the receptor.

Methods

1. Molecular Docking

The interaction between the caffeine molecule and the gelling agent polymer, as well as the CA membrane have been calculated using a molecular docking approach. [15] The target structures were set as rigid, not able to change their spatial shape, while rotatable bonds were allowed in ligands.

The 3D structure of a ligand caffeine molecule, which is a relatively small molecule, was optimized using the Density-functional theory (DFT) method [16] incorporated into the GAUSSIAN09 software [17].

Table 1. Gelling agents used in the study

INCI name	Chemical category	pH range suggested by supplier	pKa value
Xanthan Gum (XG)	Natural anionic polysaccharide [5]	2 - 12	3.1 [6]
Hydroxyethyl Cellulose (HEC)	Mixture of unsubstituted and substituted cellulose, non-ionic linear polysaccharide [7]	High pH tolerance	Non-ionic, pKa not applicable [8]
Sodium Carboxymethyl Cellulose (NaCMC)	Cellulose derivative, anionic linear polysaccharide [9]	>3.5	4.84 [10]
Carrageenan (Carr)	Natural anionic linear polysaccharide [11]	> 4	~2 [12]
Sodium Polyacrylate (NaPA)	Synthetic anionic linear sodium salt of polyacrylic acid [13]	High pH tolerance	4.5 [14]
Guar Gum (GG)	Natural non-ionic polysaccharide [5]	High pH tolerance	Non-ionic, pKa not applicable [8]

The chemical structures of gelling agents were obtained through available supplier information. Since the method requires optimised 3D structures, this was achieved by using the Molecular Mechanics/Universal Force Field (MM/UFF) method [18]. Na^+ ions dissociate from NaCMC and NaPA in aqueous solutions. Caffeine and membrane interact with CMC and PA polyanions. NaCMC and HEC contain substitutional isomers with substituents in identical positions: mono-substituted on C2 (C2-CMC and C2-HEC), C3 (C3-CMC and C3-HEC) and C6 (C6-CMC and C6-HEC) positions; di-substituted on C2 and C3 (C2,3-CMC and C2,3-HEC), C2 and C6 (C2,6-CMC and C2,6-HEC) and C3 and C6 (C3,6-CMC and C3,6-HEC) positions; tri-substituted on C2, C3 and C6 (C2,3,6-CMC and C2,3,6-HEC) positions. The optimised structures of all substitutional isomers were prepared, and averaged structural units suggested by supplier information were considered. Alpha helix of ι -Carr single chain was prepared by deleting coordinates of one chain from double-chained ι -Carr structure (pdb code: 1CAR). The remaining ι -Carr structure was optimised. The optimised structures of caffeine, CA membrane and gelling agents were then prepared for molecular docking studies. The membrane structure was optimised and selected as four mutually

sheared chains, with three different possibilities of binding, namely, gelling agent molecules attaches between and alongside the membrane chains, as well as transversally.

Two sets of docking calculations were performed using Autodock Vina [19]. In the first set, the active ingredient caffeine, as a ligand, was docked on the gelling agents and CA membrane as targets. In the second set of docking studies, the extracted parts of gelling agents that interacted with caffeine from initial computations were docked on CA membrane as the target. Receptor-ligand adducts were visualized by Mercury software [20] and analysed in BIOVIA Discovery Studio [21]. The charges of molecules, obtained through pKa values, were essential for modelling interactions between gelling agents and caffeine.

2. Preparation of Hydrogels

Six hydrogels were formulated using carrageenan (Carr), guar gum (GG), hydroxyethyl cellulose (HEC), sodium carboxymethyl cellulose (NaCMC), sodium polyacrylate (NaPA) or xanthan gum (XG) as the gelling agent, in the concentrations shown in Table 2.

Table 2 Compositions of hydrogel formulations

Ingredient	% w/w					
	XG gel	HEC gel	NaCMC gel	Carr gel	NaPA gel	GG gel
Aqua	q.s. 100					
Caffeine	2.0					
Methylparaben	0.5					
Gelling agent	3.2	1.4	2.7	2.3	1.0	1.2

Caffeine and methylparaben powders were dissolved in the deionised water under heating at 40 °C and stirring at low speed (100-200 rpm) with a hotplate/magnetic stirrer (MS-Serie, Timstar, UK). After the mixture of powders was fully dissolved, the gelling agent was slowly added into the solution under mixing, until obtaining a homogeneous dispersion, which was then cooled to room temperature with slow-speed mixing. The pH value was measured and adjusted with the citric acid solution to 5.5, if necessary. The hydrogels were left in a cool and dark place for 24 h before any characterisation tests were conducted.

3. Rheological Characterisation

Rheological properties of the hydrogels were tested with Haake Rheometer (MARS iQ Air, Thermo Scientific, Germany). The measuring geometry was a set of serrated parallel plates of 35 mm diameter, with the measuring gap of 1 mm. The sample hood was used on all tests to minimize water evaporation. All data obtained were processed with Haake RheoWin Data Manager 4.88 software (Thermo Scientific, USA). Two types of rheological tests were performed: the shear rate sweep from 10 - 200 s⁻¹ at 32 °C and the oscillatory stress sweep from 1 - 500 Pa at 32 °C at the constant frequency of 1 Hz. The linear viscoelastic region (LVR) was identified using the built-in function from RheoWin Data manager. The yield stress value was detected as the stress at which a 10% reduction in elastic modulus G' was reached.

4. 3D design and Printing

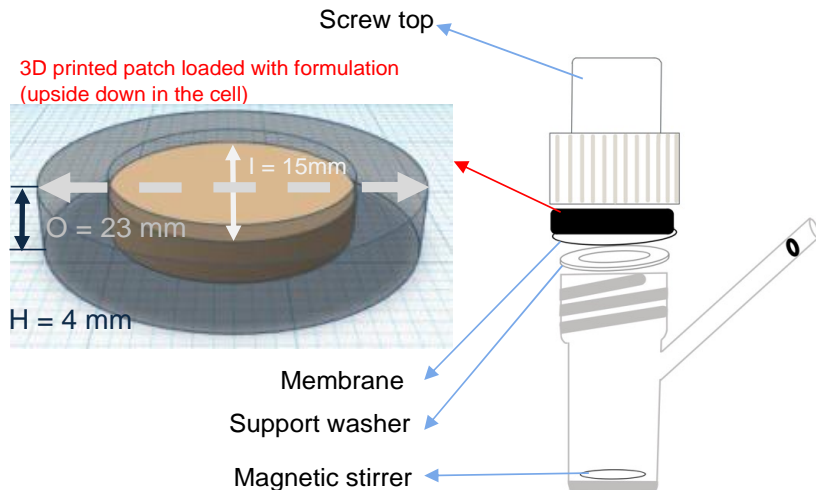


Figure 1 Schematic diagram of the Franz cell set up and 3D model of the 3D printed patch

The skin patches samples were designed with TinkerCAD web application (Autodesk, United States), to fit the vertical diffusion cells used to perform in vitro release test (IVRT). The dual-extrusion patches were composed of two materials, inert PLA as a solid holder (dark region in Figure 1) and swellable PVA as an insert, onto which the formulation would be loaded (light brown part in Figure 1). The other patch type was made of single material, PLA. The total height of the patch (H) was kept at 4 mm, so that the patch could fit into the donor

compartment of the Franz diffusion cell and be tightly screwed onto the receptor. The outer diameter was 23 mm, and inner diameter 15 mm, to fit the size of the occlusion ring used for fixing the membrane into position. The height of the insert PVA, when present, was 1 mm. An indentation of 1 mm in the patches was designed to accommodate the formulation. The patch models were processed using the Ultimaker Cura 4.9.1 software and printed with the Ultimaker S3 printer (Ultimaker, Netherlands), using a fused deposition modelling (FDM) 3D printing process. The PLA filament printing temperature was set at 210 °C and the PVA filament was printed at 215 °C.

5. IVRT

In vitro release tests (IVRT) were performed at 32 °C to mimic skin surface temperature (Thakker and Chern, 2003), with a constant stirring speed of 600 rpm, using Vertical Diffusion Cell Test System Model HDT 1000 (Copley ScientificTM, UK). Franz cells used in the experiment had a diffusion area of ~1.77 cm² and a volume of 12 mL. Pre-wetted cellulose acetate (CA) membrane was used between the two compartments. The receptor fluid was phosphate buffered saline (PBS; pH = 7.4). At specified time intervals, 500 µL of the sample was extracted and analysed by the NanoDrop™ 2000 spectrophotometer (Thermo Fischer Scientific, United States), using a previously constructed calibration curve for the absorption (λ_{max}) of caffeine recorded at 273 nm ($R^2 = 0.999$). The donor compartment was refilled with the same amount of fresh buffer solution after each sampling.

IVRT was firstly performed on the PLA patches without the PVA insert. The hydrogel formulation was loaded into to the PLA holder with 1 mm indentation. Since PLA is an inert polymer, it was assumed that it would not interact with the formulation. The loaded patch was then fixed into the donor compartment with the hydrogel facing the membrane, as shown in Figure 1 (right). 150 mg of hydrogel was loaded onto 3D printed patch and placed under room temperature for 45 mins. The loaded patch was then inserted to the donor compartment of the Franz cell and start the IVRT, with sampling times at 0.5 h, 1 h, 2 h, 3 h, 5 h and 6 h. The same procedure was applied when the PVA-PLA patches were used. The results are reported as % release, which was calculated as the cumulative amount of drug released at

time t over the initial amount of caffeine in ~150 mg of hydrogel formulation. [22] Five repeats were carried out for each hydrogel in both test conditions.

6. Statistical Analysis

Two sets of One-Way analysis of variance (ANOVA) tests were performed for each type of patch, using SPSS 28.0 (IBM, Armonk, NY, USA) on the caffeine release results obtained from IVRT: at 1 hour and 6 hours. The assumptions included the independence of observations, while the equality of variance across predictors was tested by Levene's test. No outliers were detected. The sample size was less than 30, thus the normality of each set of samples was also tested. The level of significance was taken as $p < 0.05$.

Results

1. Molecular Docking Analysis

The calculated binding energies obtained from molecular docking are summarised in Table 3. The new parameter ΔE was calculated as the difference between the affinity of each hydrogel towards the membrane and its affinity towards caffeine.

Table 3 Results of the molecular docking calculations of the binding energy between gelling agents and the CA membrane and caffeine, respectively

Gelling agent	Binding energy (kcal/mol) towards		ΔE (kcal/mol)
	CA membrane	Caffeine	
XG	-6.3	-4.1	-2.2
NaCMC	-5.3	-3.1	-2.2
Carr	-6.0	-3.7	-2.3
NaPA	-4.1	-2.4	-2.3
HEC	-5.7	-3.4	-2.3
GG	-6.8	-4.3	-2.5

The negative signs indicate that all interactions were attractive. A higher absolute value shows stronger attraction. The docking calculations of the binding energy between ligand caffeine and the polymer of the CA membrane have shown that the interaction between caffeine and CA membrane was -5.0 kcal/mol.

The gelling agents differ chemically and structurally, NaCMC, HEC and Carr gelling agents are linear polymers with various substituents, whereby only HEC remains neutral in the formulation and PBS. GG is a branched polymer without substituents. NaPA is linear unsubstituted macromolecule, existing in a polyanionic state under the experimental conditions. XG polymer is also branched. From the docking study results, it could be concluded that caffeine has a higher binding energy for branched targets or targets with substituents than for linear gelling agents, as shown in Table 3. Also, compared to neutral thickeners, negatively charged thickeners had lower affinity towards caffeine. NaPA, the only synthetic polymer, had the lowest binding energy, since it could not form hydrogen bonds with caffeine.

Through visual inspection of the results, it could be concluded that gelling agents are bound between two membrane chains, without any transversal attachment. The docking calculations on the membrane structure showed that gelling agents had higher affinity towards the membrane than towards caffeine. This affinity was also higher than caffeine affinity towards membrane. Hence, it can be expected that the new supramolecular structures composed of gelling agents and membrane chains form upon the contact of hydrogels to the membrane during IVRT.

In addition, the difference between caffeine-gelling agent and gelling agent-membrane interactions (ΔE) are very close, so the type of gelling agent will not have a significant influence on the release of caffeine. The CA membrane attracts both gelling agents and caffeine. All caffeine-gelling agent interactions are weaker than that for caffeine-CA membrane, which indicates that the active molecule will eventually leave the formulation.

2. Rheological Characterisation

The viscosity curves of six hydrogels are shown in Figure 2. All formulations possessed shear-thinning behaviour, as viscosity progressively decreased under increased shear, due to the fact that the polymeric chains in the gelling agents align in the direction of shear. At high shear rates, the viscosity tends to be constant since no further disruption of the structure could occur. All hydrogels have shown similar flow behaviour (Figure 2), with NaPA having the highest viscosity over the whole shear rate range, GG, HEC and XG were in the middle, while the viscosity of NaCMC and Carr were the lowest. Complex modulus G^* , also known as rigidity, is a direct measure of the balance between viscous and elastic components, which are expressed as viscous (G'') and elastic (G') moduli. The visualisation and mathematical relationship between the three moduli are shown in Figure 3. Thus, G^* expresses the balance between the liquid-like and the solid-like behaviour under oscillatory stress conditions. Figure 4 shows the changes in rigidity of each hydrogel with increasing oscillatory shear stress. The first, flat part of the curve, signifies the linear viscoelastic region (LVR) where rigidity does not depend on the applied stress. As the stress increases, at some point the rigidity starts to decrease, indicating the yield region and the breakdown of the internal structure. The yield stress value was identified as a 10% reduction in G' from the LVR value.

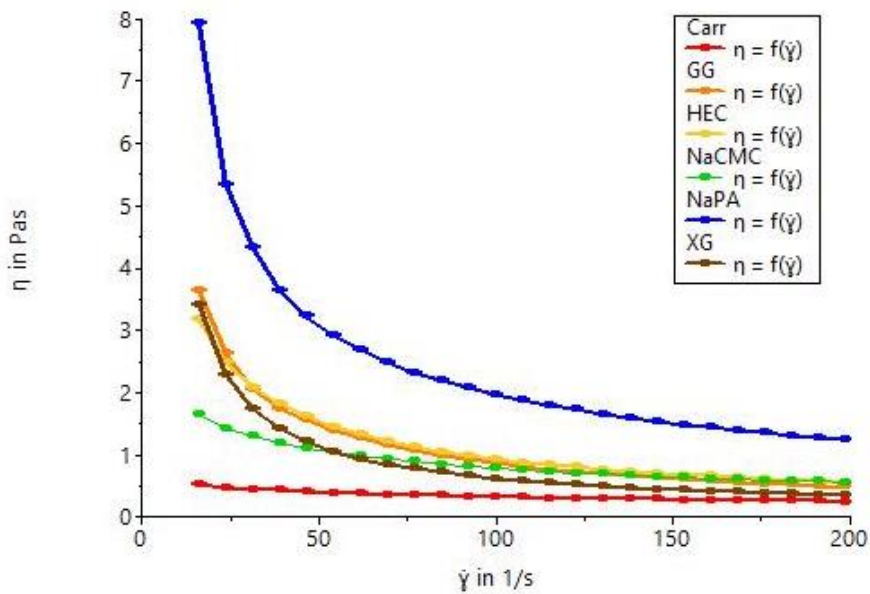


Figure 2 Changes in viscosity of the six hydrogels during the shear rate sweep (10 - 200 1/s at 32 °C)

$$\tan \delta = \frac{G''}{G'}$$

$$G' = G^* \cos \delta$$

$$G'' = G^* \sin \delta$$

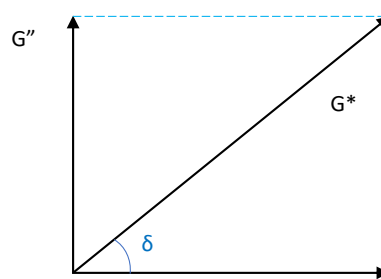


Figure 3 Relationship between complex modulus G^* , elastic modulus G' and viscous modulus G''

Table 4 summarises the results obtained from the shear rate sweep (including viscosity values obtained at high and low shear rate, respectively) and the oscillatory stress sweep (including elastic modulus at LVR and yield stress). It can be seen that NaCMC and Carr were predominantly liquid-like semisolids with no identifiable yield point, while NaPA had the highest elastic properties (G') and the strongest internal structure (yield point).

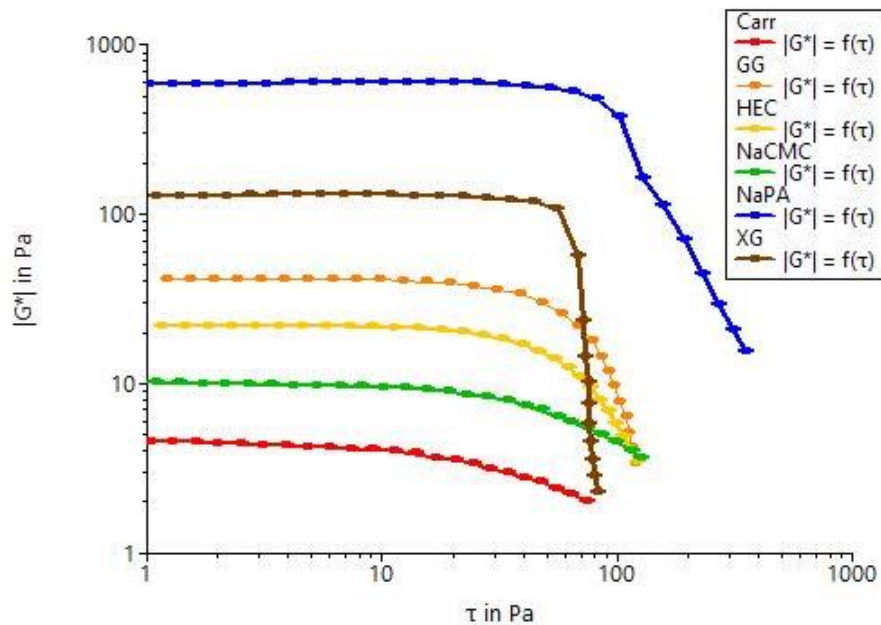


Figure 4 Changes in the complex modulus G^* of the six hydrogels during the oscillatory stress sweep (1 - 500 Pa at 1 Hz) at 32 °C.

Table 4 Key values obtained from rheological tests

Gelling agent	Conc. (% w/w)	Shear rate sweep (Figure 3)		Oscillatory stress sweep (Figure 4)	
		Viscosity at of 16 s ⁻¹ (Pa s)	Viscosity at of 190 s ⁻¹ (Pa s)	Elastic modulus (Pa)	Yield stress (Pa)
Carr	2.3	0.527	0.2615	No LVR	Liquid, no yield
GG	1.2	3.638	0.5037	33.76	23.21
HEC	1.4	3.17	0.5847	21.64	26.65
NaCMC	2.7	1.652	0.5759	No LVR	Liquid, no yield
NaPA	1.0	7.936	1.280	589.7	60.11
XG	3.2	3.404	0.3684	125.6	43.82

3. IVRT and Statistical Analysis

The results obtained from the IVRT analysis of the hydrogels applied on the inert PVA insert and on the swellable PVA insert are presented in Figures 5 and 6, respectively. Figure 5 indicates that the initial caffeine release from Carr and XG was lower than from the other hydrogels. It can also be seen that the release from all hydrogels reached a constant level after 3 hours and was the lowest from Carr.

Two One-Way Repeated Measures ANOVA tests were performed on the data, after one and 6 hours of release, respectively. The null hypothesis in both cases was that there was no statistically significant difference in the caffeine release among the six hydrogels. There were no outliers and the tests for normality showed that the data were normally distributed in all cases.

ANOVA analysis after one hour of release showed a statistically significant difference in the release from different hydrogels, $F(5, 24) = 7.872$; $p = 0.001$. Bonferroni post-hoc test revealed significant differences between Carr and NaPA, Carr and XG and between HEC and NaPA.

ANOVA analysis after 6 hours showed a statistically significant difference in the release from different hydrogels, $F(5, 24) = 22.111$; $p < 0.001$. Bonferroni post-hoc test revealed significant differences between GG and XG, HEC and NaPA, Carr against GG, HEC and NaCMC.

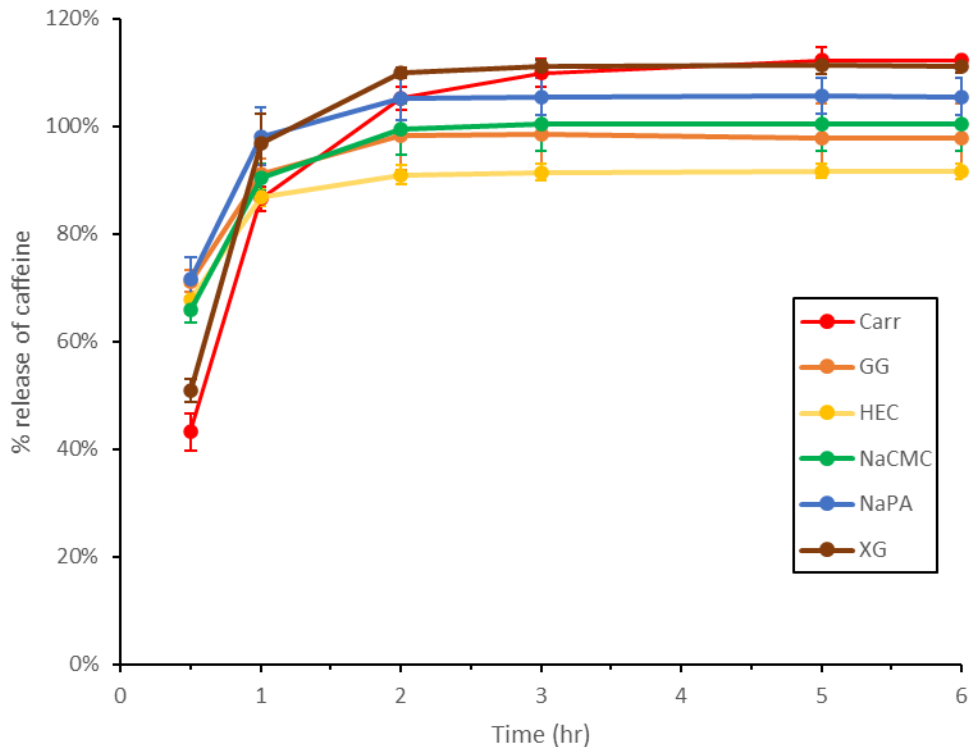


Figure 5 Release profiles of 6 hydrogels applied on the inert PLA patch: standard deviation was added as error bars.

Figure 6 shows the release profiles when the combination of PVA with a swellable PLA patch was loaded by the tested hydrogels. The initial release was slower in comparison with Figure 5, which was due to the presence of another hydrophilic polymer (PVA) in the patch. It is noticeable that none of the hydrogels have reached 100%, nor they have plateaued after 6 hours of IVRT.

ANOVA analysis after one hour of release showed a statistically significant difference in the release from different hydrogels, $F(5, 24) = 3.799$, $p = 0.011$. Bonferroni post-hoc test showed that the only significant difference was between NaCMC and GG.

ANOVA analysis after 6 hours showed a statistically significant difference in the release from different hydrogels, $F(5, 24) = 6.021$, $p = 0.001$. Bonferroni post-hoc test showed that the only significant difference was between HEC and GG.

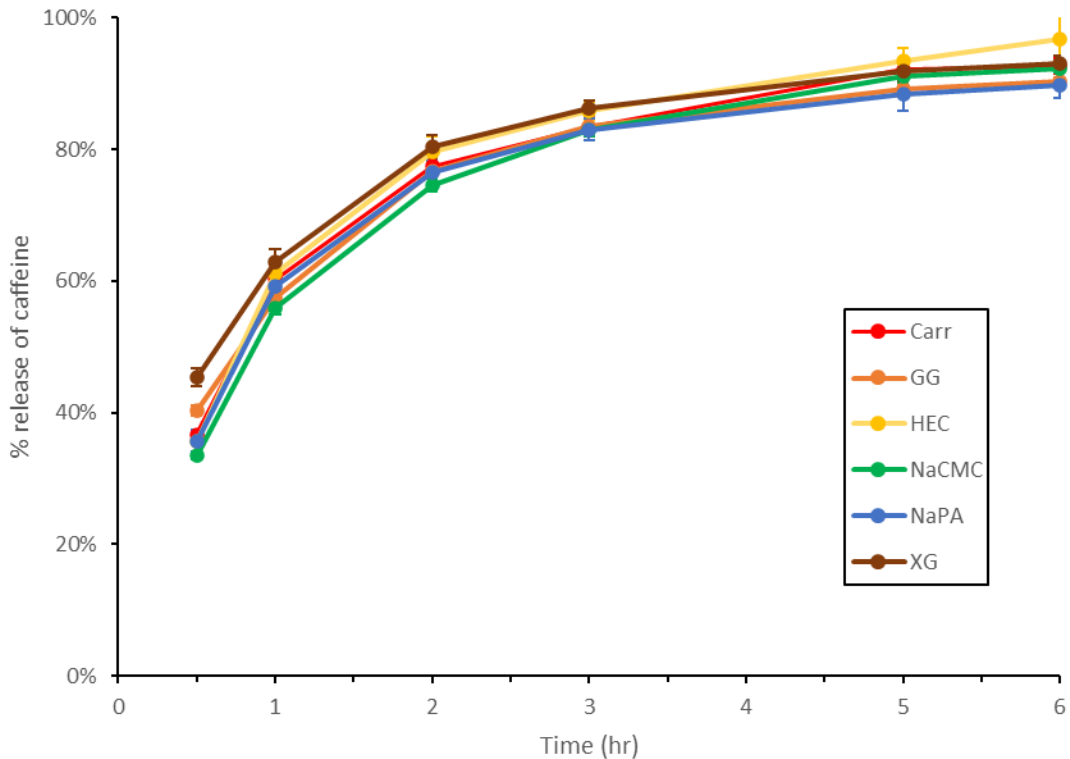


Figure 6 Release profiles of the 6 hydrogels applied on the swellable PLA patch: standard deviation was added as error bars.

Discussion

The six hydrogels used in this study had similar viscosity profiles (Figure 2), but with some differences which could be used to divide them into higher viscosity (NaPA), medium viscosity (GG, HEC and XG) and lower viscosity group (Carr and NaCMC). Theoretically, the release rate of an active ingredient should be lower for high viscosity semisolids [2]. It was of interest to determine whether the small differences in viscosity and yield value would be reflected in differences in release profiles, under the conditions of IVRT. The results

showed (Figure 5) that the differences were small, although some of them were significant, the pattern did not strictly follow the above rheological differences.

However, the most interesting aspect of this study was the comparison between the theoretically predicted and experimentally tested caffeine release from the six hydrogels. The MD analysis (Table 3) showed that the caffeine–membrane interactions were stronger than caffeine–GA interactions, therefore, it could be expected that the overall intermolecular forces would lead to the diffusion of caffeine from the hydrogel and its interaction with the membrane. The affinity of active molecules towards the gelling agents hinders the release. However, in the competition between the gelling agents and caffeine towards the membrane, gelling agents have higher affinity, which should lead to the caffeine diffusion into PBS, due to weaker binding.

The rate of caffeine release depended on the permeability of caffeine through the newly formed gelling agent–membrane system, as well as the membrane pore size, the latter of which was not considered in these calculations in order to simplify the system. According to calculations, gelling agent polymers tended to bind between membrane chains (not transversally), which largely hinder the path of caffeine, hence the rate of caffeine release into the PBS will depend on the number and length of the gelling agent chains. Therefore, the initial mass of polymers may affect the release of caffeine. Increasing the concentration of gelling agent in the formulation would lead to more pores of membrane being occupied, resulting in reduced caffeine permeability.

When the PVA-PLA patches were used, the release of caffeine was notably reduced from that detected from the PVA-only patches (Figures 5 and 6), since hydrogel formulations interacted with the hydrophilic PVA insert. Since PVA was swelling due to the presence of water in the formulation, it is assumed that some caffeine molecules entered the PVA polymer network and were retained, leading to a lower release over time (Figure 6).

When the inert PLA patches were used, however, the situation was equivalent to the release from the formulation under occlusion, leading to more pronounced differences in release rates than in the presence of PVA (Figure 5). Apart from small rheological differences,

another factor affecting release could be the presence of bound water in the polymer network, which was not considered in the molecular docking calculations. Some caffeine molecules may not have been attached to the gelling agents as assumed in the MD, but interacted with the non-bound water, and were more available to leave the formulation [23]. This could be further investigated by different methods, e.g. TGA and Raman spectroscopy, to establish how water molecules in the formulation affect the release of caffeine.

Further developments in the MD direction should consider the presence of PVA, aiming to investigate the mechanism of hindered caffeine release, with the intention of producing a controlled-release system. Molecular dynamics is another powerful computational tool which could be employed, providing information on the molecular behaviour over time, which is directly relevant to the *in vitro* and *in vivo* release of cosmetic active ingredients.

Conclusion

The aims of the present study were to determine the feasibility of using molecular docking calculations to predict the release of active ingredients and to provide a better understanding of the release mechanisms. Promising initial results were obtained, providing a ‘proof of concept’. It was shown that molecular docking could partly explain how the chemical structure of gelling agents affects the release of caffeine from the hydrogels, loaded on two types of 3D-printed skin patches.

In common with other theoretical models, molecular docking suffers from over-simplifying the complex system of cosmetic active release. It is not likely to become a stand-alone solution for designing effective cosmetic formulations but, with further method development, it has the potential to assist researchers in the selection of excipients for the given active ingredient.

Acknowledgments. NONE.

Conflict of Interest Statement. NONE.

References

1. Mitura, S., Sionkowska, A., & Jaiswal, A. (2020). Biopolymers for hydrogels in cosmetics: review. *Journal of Materials Science. Materials in Medicine*, 31(6) doi:10.1007/s10856-020-06390-w
2. Li, J., & Mooney, D. J. (2016). Designing hydrogels for controlled drug delivery. *Nature Reviews. Materials*, 1(12) doi:10.1038/natrevmats.2016.71
3. Singh, S., Bani Baker, Q., & Singh, D. B. (2022). Chapter 18 - Molecular docking and molecular dynamics simulation. In D. B. Singh, & R. K. Pathak (Eds.), *Bioinformatics* (pp. 291-304) Academic Press. Retrieved from <https://www.sciencedirect.com/science/article/pii/B9780323897754000146>
4. Salmaso, V., & Moro, S. (2018). Bridging Molecular Docking to Molecular Dynamics in Exploring Ligand-Protein Recognition Process: An Overview. *Frontiers in Pharmacology*, 0 doi:10.3389/fphar.2018.00923
5. Parente, M. E., Ochoa Andrade, A., Ares, G., Russo, F., & Jiménez-Kairuz, A. (2015). Bioadhesive hydrogels for cosmetic applications. *International Journal of Cosmetic Science*, 37(5), 511-518. doi:10.1111/ics.12227
6. Oprea, A., Nistor, M., Profire, L., Popa, M. I., Lupusoru, C. E., & Vasile, C. (2013). Evaluation of the Controlled Release Ability of Theophylline from Xanthan/Chondroitin Sulfate Hydrogels. *Journal of Biomaterials and Nanobiotechnology*, 4(2), 123-131. doi:10.4236/jbnb.2013.42017
7. Lambson Limited. (2017, Product Range High Performance Ingredients for Personal Care Formulations., 12. Retrieved from www.lambson.com
8. Afzaal, M., Saeed, F., Ahmed, A., Saeed, M., & Ateeq, H. (2022). Chapter 21 - Hydrogels as carrier for the delivery of probiotics. In J. Singh, & A. Vyas (Eds.), *Advances in Dairy Microbial Products* (pp. 303-315) Woodhead Publishing. Retrieved from <https://www.sciencedirect.com/science/article/pii/B9780323857932000199>

9. Li, W., Sun, B., & Wu, P. (2009). Study on hydrogen bonds of carboxymethyl cellulose sodium film with two-dimensional correlation infrared spectroscopy. *Carbohydrate Polymers*, 78(3), 454-461. doi:10.1016/j.carbpol.2009.05.002
10. Kumar, A., Singh, K., Bhat, R. A., & Dixit, U. (2021). Interpretation of adsorption behaviour of cellulose, sodium carboxymethylcellulose and hydroxyethylcellulose onto activated kaolin. *JCIS Open*, 3, 100017. doi:10.1016/j.jciso.2021.100017
11. Cheng, H., Zhang, X., Cui, Z., & Mao, S. (2021). *Grafted polysaccharides as advanced pharmaceutical excipients* Elsevier Inc. Retrieved from <http://dx.doi.org/10.1016/B978-0-12-820043-8.00010-4>
12. Gu, Y. S., Decker, E. A., & McClements, D. J. (2004). Influence of pH and iota-carrageenan concentration on physicochemical properties and stability of beta-lactoglobulin-stabilized oil-in-water emulsions. *Journal of Agricultural and Food Chemistry*, 52(11), 3626-3632. doi:10.1021/jf0352834
13. Chang, Z., Chen, Y., Tang, S., Yang, J., Chen, Y., Chen, S., . . . Yang, Z. (2020). Construction of chitosan/polyacrylate/graphene oxide composite physical hydrogel by semi-dissolution/acidification/sol-gel transition method and its simultaneous cationic and anionic dye adsorption properties. *Carbohydrate Polymers*, 229, 115431. doi:10.1016/j.carbpol.2019.115431
14. Swift, T., Swanson, L., Geoghegan, M., & Rimmer, S. (2016). The pH-responsive behaviour of poly(acrylic acid) in aqueous solution is dependent on molar mass. *Soft Matter*, 12(9), 2542-2549. doi:10.1039/C5SM02693H
15. Morris, G. M., & Lim-Wilby, M. (2008). Molecular Docking. *Methods in molecular biology (Clifton, N.J.)* (pp. 365-382). Totowa, NJ: Humana Press. Retrieved from http://link.springer.com/10.1007/978-1-59745-177-2_19
16. Engel, E., & Dreizler, R. M. (2011). *Density functional theory* (1. Aufl. ed.). Heidelberg [u.a.]: Springer. Retrieved from http://bvbr.bib-bvb.de:8991/F?func=service&doc_library=BVB01&local_base=BVB01&doc_number

[=020801741&sequence=000001&line_number=0001&func_code=DB_RECORDS&service_type=MEDIA](#)

17. M. J. Frisch, G. W. Trucks, H. B. Schlegel, G. E. Scuseria, M. A. Robb, J. R. Cheeseman, G. Scalmani, V. Barone, G. A. Petersson, H. Nakatsuji, X. Li, M. Caricato, A. Marenich, J. Bloino, B. G. Janesko, R. Gomperts, B. Mennucci, H. P. Hratchian, J. V. Ortiz, A. F. Izmaylov, J. L. Sonnenberg, D. Williams-Young, F. Ding, F. Lipparini, F. Egidi, J. Goings, B. Peng, A. Petrone, T. Henderson, D. Ranasinghe, V. G. Zakrzewski, J. Gao, N. Rega, G. Zheng, W. Liang, M. Hada, M. Ehara, K. Toyota, R. Fukuda, J. Hasegawa, M. Ishida, T. Nakajima, Y. Honda, O. Kitao, H. Nakai, T. Vreven, K. Throssell, J. A. Montgomery, Jr., J. E. Peralta, F. Ogliaro, M. Bearpark, J. J. Heyd, E. Brothers, K. N. Kudin, V. N. Staroverov, T. Keith, R. Kobayashi, J. Normand, K. Raghavachari, A. Rendell, J. C. Burant, S. S. Iyengar, J. Tomasi, M. Cossi, J. M. Millam, M. Klene, C. Adamo, R. Cammi, J. W. Ochterski, R. L. Martin, K. Morokuma, O. Farkas, J. B. Foresman, and D. J. Fox. (2016). Gaussian 09, Revision A.02 [computer software]. Gaussian, Inc., Wallingford CT:
18. Rappe, A. K., Casewit, C. J., Colwell, K. S., Goddard, W. A., & Skiff, W. M. (1992). UFF, a full periodic table force field for molecular mechanics and molecular dynamics simulations. *Journal of the American Chemical Society*, 114(25), 10024-10035. doi:10.1021/ja00051a040
19. Trott, O., & Olson, A. J. (2010). AutoDock Vina: Improving the speed and accuracy of docking with a new scoring function, efficient optimization, and multithreading. *Journal of Computational Chemistry*, 31(2), 455-461. doi:10.1002/jcc.21334
20. Macrae, C. F., Sovago, I., Cottrell, S. J., Galek, P. T. A., McCabe, P., Pidcock, E., . . . Wood, P. A. (2020). Mercury 4.0: from visualization to analysis, design and prediction. *Journal of Applied Crystallography*, 53(1), 226-235. doi:10.1107/S1600576719014092
21. [Discovery Studio Visualizer]. (2015). BIOVIA, Dassault Systèmes [computer software]. San Diego: Dassault Systèmes:

22. Mughal, M. A., Iqbal, Z., & Neau, S. H. (2010). Guar Gum, Xanthan Gum, and HPMC Can Define Release Mechanisms and Sustain Release of Propranolol Hydrochloride. *AAPS PharmSciTech*, 12(1), 77-87. doi:10.1208/s12249-010-9570-1
23. De Vivo, Masetti, Bottegoni, & Cavalli. (2016). Role of Molecular Dynamics and Related Methods in Drug Discovery. *Journal of Medicinal Chemistry*, 59(9), 4035-4061. doi:10.1021/acs.jmedchem.5b01684